Determination of the crystal-field splitting of the $4f^1$ state in samarium-alloyed cerium hexaboride

Gan Zhao,[1] Huayao Li,[1] Wenting Lin,[1] Quan Ren,[1] Jonathan Denlinger,[2] Yi-De Chuang,[2] Xiaoqian Zhang,[3] L. Andrew Wray,[4,†] and Lin Miao[1,*]

[1]*Key Laboratory of Quantum Materials and Devices of Ministry of Education, School of Physics, Southeast University, Nanjing 211189, China*
[2]*Advanced Light Source, Lawrence Berkeley National Laboratory, Berkeley, California 94720, USA*
[3]*International Quantum Academy, Shenzhen 518048, China*
[4]*Department of Physics, New York University, New York, New York 10003, USA*

(Received 3 May 2023; revised 11 June 2023; accepted 12 June 2023; published 30 June 2023)

The cerium hexaboride and its alloyed compounds are strongly correlated materials, hosting many-body hidden order or nontrivial band topology. The fine electronic structure of the Ce $4f^1$ state, derived from spin-orbit coupling and crystal electric field splitting (CEF), plays a vital role in forming the exotic quantum state in Ce-based compounds. By using the high-resolution resonant inelastic x-ray scattering technique, we determined the fine electronic excitation energies of the Ce $4f^1$ state in the Kondo material $Ce_{0.3}Sm_{0.7}B_6$. The extracted energy levels show an overall consistency with other scattering techniques, except that CEF splitting in the total angular momentum $J = 7/2$ state is identified to be (89.5 ± 1) meV, clearly larger than the value of 82 meV drawn from Raman spectroscopy. A detailed discussion is made to reconcile the mismatch. This work provides key information on the Ce $4f^1$ orbital in CeB_6, which would also put a constraint on the related theoretical model, helping to address the challenges for theoretical dealings with many-body correlations in Ce $4f^1$ compounds.

DOI: 10.1103/PhysRevB.107.245149

I. INTRODUCTION

Ce-based compounds have been intensively studied due to their many-body interactions and the intertwined coupling between different degrees of freedom [1–6]. A stable trivalent Ce ion has an outer shell of $4f^1$. Strong spin-orbit coupling (SOC), a high susceptibility to ordered magnetism, and an intrinsic Kondo effect within the Ce $4f^1$ state make its compounds a fertile ground of electronic correlation and quantum criticality [7,8]. For instance, Ce-based materials such as $CeCu_2Si_2$ and $CeCoIn_5$ are archetypical heavy fermion superconductors [9–11]. The Ce $4f^1$ state also dominates dense Kondo behavior in $Ce_xLa_{1-x}Cu_6$ [12,13] and $Ce_xLa_{1-x}Ni_2Ge_2$ [14]. Among these correlated materials, CeB_6 and its alloyed derivatives such as $Ce_{1-x}La_xB_6$ attract particular interest due to their unique properties [15–19]. CeB_6 possesses a cubic lattice under the space group of $Pm3m$. Ce atoms form the frame of a cube which is centered by an octahedral (O_h) boron cage [Fig. 1(a)]. The Ce site can be substituted with other metallic lanthanides such as La/Sm/Eu, transforming it to a different quantum phase without altering the crystal structure [20–23]. CeB_6 has been found to host a "hidden order" at a temperature between 2.4 and 3.2 K, which is proposed as a result of the magnetic multipolar effect but is still under debate [24–26]. Despite strong evidence for the existence of many-body quantum order, recent work reported that substituting Ce with Sm could achieve nontrivial topology in $Ce_{1-x}Sm_xB_6$ ($x > 0.5$), which is known as a topological Kondo system [27,28].

Regardless of the hidden order or the topological Kondo phase, those exotic properties of CeB_6 and its alloyed compounds strongly rely on the energy levels in the vicinity of the Fermi level and the associated ground state symmetries [28,29]. Massive efforts have been taken to determine the ground state of Ce $4f^1$ [30,31], and an overview can be achieved [Fig. 1(b)]. Strong SOC splits the $4f^1$ state into $4f_{7/2}$ and $4f_{5/2}$, in which $4f_{5/2}$ is ~270 meV lower in energy [32]. Within the crystal electric field (CEF) of O_h symmetry, the sixfold degenerate $4f_{5/2}$ states are further split into different symmetries of Γ_8 and Γ_7. Neutron scatterings and x-ray spectroscopy studies have claimed a CEF in $4f_{5/2}$ as ~50 meV, and it is now widely acknowledged that quadruplet Γ_8 is the ground state after a long debate [8,33]. There are also first-principles calculations aiming to reveal the splitting within Ce $4f_{7/2}$ under various CEF symmetries, suggesting an energy hierarchy of Γ_6', Γ_8', and Γ_7' symmetries and their relative energy spacing of ~100 meV (under a tetragonal lattice) [30]. However, most experimental studies focus on the lower branch ($J = 5/2$) of the SOC split $4f^1$ state [8,20,29,34], and the direct measurement of CEF splitting in an upper branch ($J = 7/2$) of CeB_6 has rarely been reported. The only experimental work based on Raman spectroscopy claims a CEF split of 82 meV in the $J = 7/2$ state, leading to a discrepancy between the experiment and numerical calculation [35]. To resolve the disputed results, we studied the $4f^1$ orbital's energy hierarchy in $Ce_{0.3}Sm_{0.7}B_6$ by using high-resolution resonant inelastic x-ray scattering (RIXS). The very fine CEF split electronic structures within the $J = 7/2$ and $J = 5/2$ states are depicted. The CEF split energy scale of $J = 7/2$ is

*Corresponding author: lmiao@seu.edu.cn
†Corresponding author: lawray@nyu.edu.cn

discovered to be (89.5 ± 1) meV, which is larger than previously reported. Our work puts a well-defined constraint on further theoretical treatment, which is a step forward to understanding the strongly correlated effect within Ce-based compounds.

II. EXPRIMENT

High-resolution x-ray absorption spectroscopy (XAS) and RIXS measurements were both performed at the beamline 4.0.3 endstation (MERIXS) at the Advanced Light Source (ALS). The incident photon energy was tuned between 100 and 150 eV to cover the $N_{4,5}$ edge ($4d^{10}4f^n$ to $4d^94f^{n+1}$ transition) of Ce or Sm. The total electron yield (TEY) mode was used in the XAS. To gain good signal statistics, the RIXS experiment was performed with π-polarized incident photons. $Ce_{0.3}Sm_{0.7}B_6$ samples are of high crystalline qualities, the same as the ones in an earlier study [27,28]. Alloying with Sm makes $Ce_{0.3}Sm_{0.7}B_6$ to be well cleaved, generating high-quality data under ultraviolet RIXS (see Supplemental Fig. S1 [36]). Large single crystals of $Ce_{0.3}Sm_{0.7}B_6$ were cleaved and measured at a low temperature (20 K), meanwhile maintained at an ultrahigh vacuum with a pressure of approximately 3×10^{-10} Torr.

III. RESULTS AND DISCUSSIONS

The $N_{4,5}$-edge XAS spectrum of the $Ce_{0.3}Sm_{0.7}B_6$ is shown in Fig. 2(a), which is also compared with the XAS of pristine CeB_6 and SmB_6. Actually, the overall spectrum is a composite of the N-edge XAS of both Ce and Sm. Unlike the main absorptive peak which is easily affected by the Fano resonance, the pre-edge peaks are not susceptible to Fano resonance but are highly sensitive to the valence state [37]. By scrutinizing the fine pre-edge peaks at around 110 eV, one could see the pre-edge peaks are almost identical between CeB_6 and $Ce_{0.3}Sm_{0.7}B_6$, indicating the trivalent nature of Ce in $Ce_{0.3}Sm_{0.7}B_6$ [Fig. 2(b)]. This confirms that alloying with Sm would not change the valence state of Ce, and vice versa. Meanwhile, atomic multiplet simulation agrees that pre-edge peaks of Ce locate well below $h\nu = 115$ eV, excluding the multiplet states from divalent and trivalent Sm (see Supplemental Fig. S2 [36]). The distinct separation of energy between the Ce N edge and Sm N edge provides an excellent opportunity to study the inelastic excitations of Ce without the inclusion of signals from Sm.

It is known that the N-edge excitation of lanthanide metal gives rise to a large cross section for inelastic x-ray scattering [39,40]. The first N-edge RIXS study on a Ce-based compound was reported decades ago, but with very limited energy resolution, and the sub-eV fine inelastic emission is not clearly identified [41,42]. The remarkable improvement of the energy resolution in RIXS now gives a chance to detect fine excitations. Figure 3(a) shows the Ce N-edge RIXS as dependent on incident photon energies. Regardless of whether the incident photons locate at the pre-edge fine peaks (from 102 to 112 eV) or at the main peaks with a higher excitation energy (>122 eV), their inelastic emissions remain almost constant in energy, in spite of the variation of intensities. Detailed photon emission line profiles are shown in Fig. 3(b), from which two

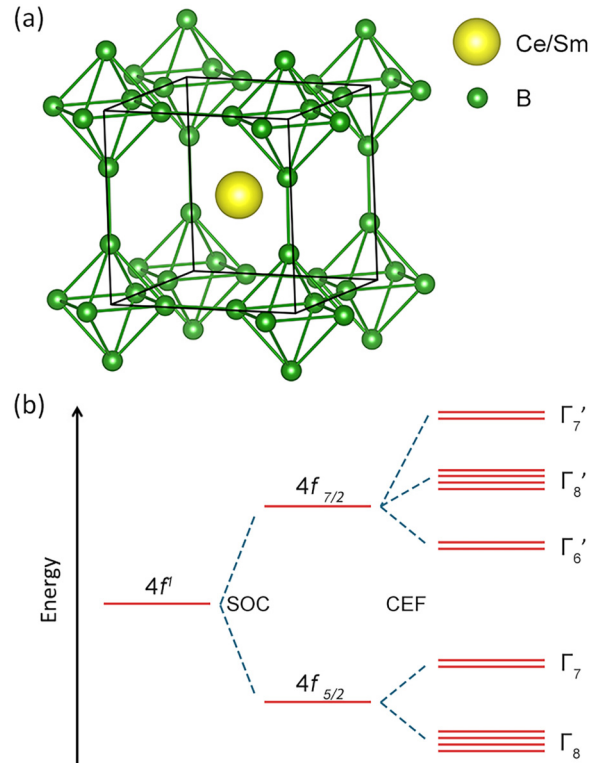

FIG. 1. (a) Crystal structure of CeB_6. (b) Schematic diagram of Ce^{3+} $4f^1$ energy levels. The $4f^1$ orbital is split into two states $4f_{7/2}$ and $4f_{5/2}$ by spin-orbit coupling (SOC). In the crystal electric field (CEF), the $J = 5/2$ states are split into two symmetries Γ_8 and Γ_7, corresponding to four- and twofold degeneracy, and the $J = 7/2$ states are split into three symmetries Γ_7', Γ_8', and Γ_6', which are of two-, four-, and twofold degeneracy, respectively.

bunches of excitation peaks can be observed at the lower and higher excitation energy. In the low-energy regime, to very close to the elastic peak, there exists an inelastic emission with a fitted energy loss of ~50 meV, namely peak 2 [Fig. 3(d)]. This excitation recalls a previously accounted CEF split energy between quadruplet Γ_8 and doublet Γ_7 in the $J = 5/2$ state, which was reported as 60 meV (photoemission [43]), 46 meV (neutron scattering [8]), and 47 meV (Raman scattering [8]). Therefore peak 2 should be attributed to the CEF excitation from Γ_8 and Γ_7. Other relatively weak excitations above 270 meV could be found by looking into the regime with a higher-energy loss [Fig. 3(c)]. This separated energy of 270 meV is coincident with the spin-orbit splitting in the $4f^1$ states [32], which indicates those excitations are spin-orbital excitations by flipping the spins from the $J = 5/2$ to $J = 7/2$ states (see Fig. 1).

As we discussed, intensive efforts have been made to understand low-energy excitations in CeB_6, but excitation with higher energy has seldom been reported and less discussed. Instead of three energy levels of symmetries (Γ_6', Γ_8', and Γ_7') predicted by the calculation, there seem to be only two peaks in the upper branch from the RIXS data [Fig. 3(c)], which is intriguing. The separation of the two peaks is approximately 80 meV, which fits precisely with CEF separation in the Raman experiment but lacks an excitation peak observed before. Assuming Γ_8' and Γ_6' of $J = 7/2$ states are located too close

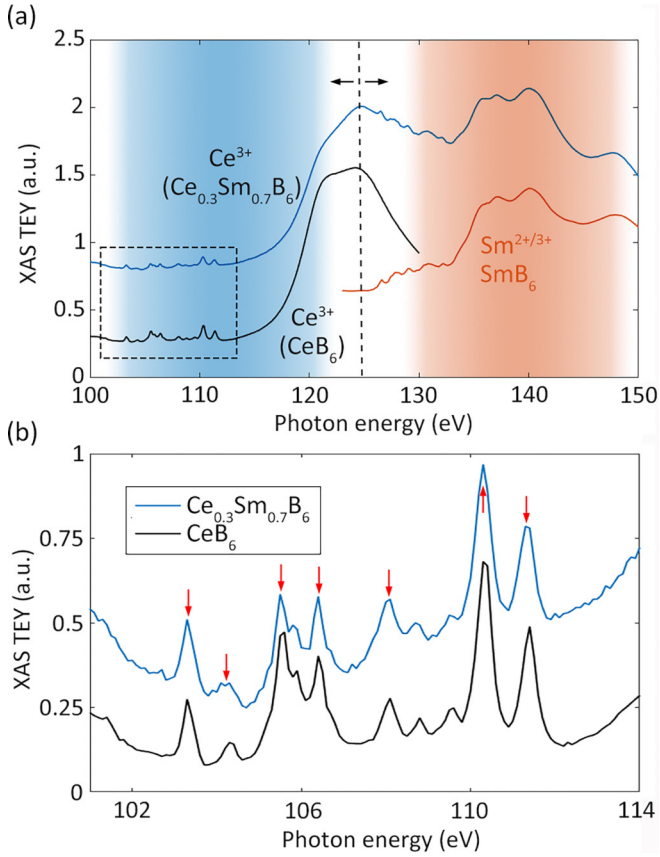

FIG. 2. (a) N-edge XAS on $Ce_{0.3}Sm_{0.7}B_6$ (blue curve), which is compared with the N-edge XAS of pristine CeB_6 (black curve, shaded with blue) and pristine SmB_6 (red curve, shaded with red). (b) The pre-edge fine peaks of Ce XAS at $h\nu < 114$ eV are compared between CeB_6 and $Ce_{0.3}Sm_{0.7}B_6$. The incident photon energies selected for the following RIXS measurements are marked by the vertical arrows.

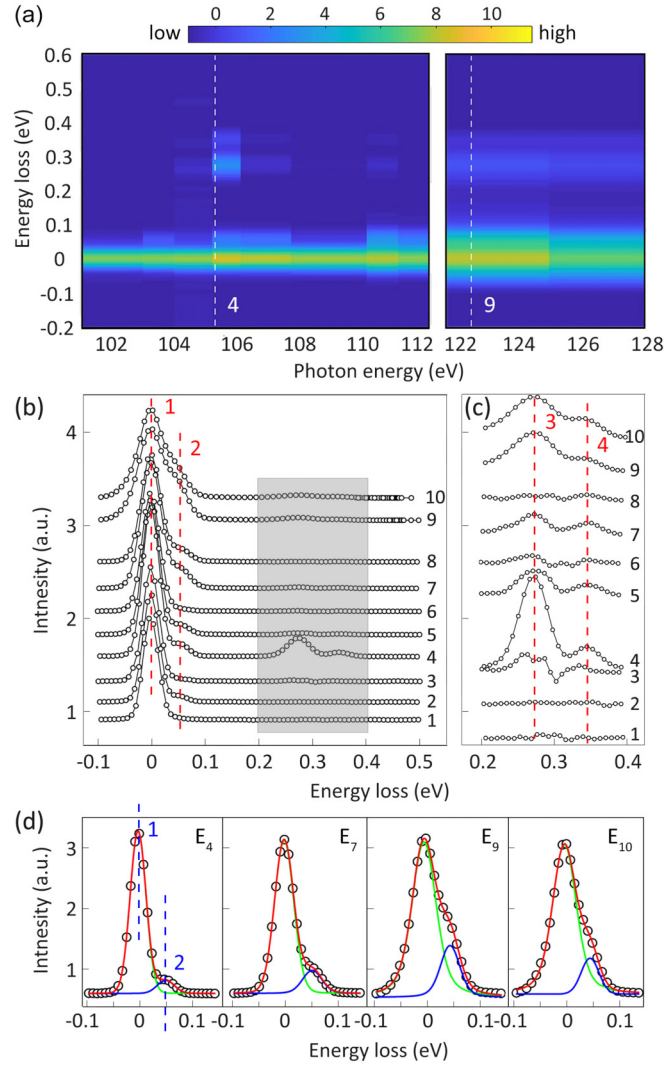

FIG. 3. (a) The Ce N-edge RIXS map is displayed as a function of the incident photon energy and the energy loss of the scattered photon. (b) The RIXS spectra sliced from the maps at ten different incident photon energies ($h\nu = 101.4$, 103.3, 104.3, 105.5, 106.4, 108, 110.4, 111.4, 122.2, and 125 eV which are labeled from E_1 to E_{10}), in which $E_4 = 105.5$ eV and $E_9 = 122.2$ eV are marked by the white dashed line in (a). The elastic peak [Γ_8 and its nearby inelastic peak (Γ_8) to Γ_7)] are marked by dashed vertical lines. (c) Magnification of the weak inelastic peaks by zooming in the gray-shaded rectangle in (b). (d) The elastic and inelastic emission of the $J = 5/2$ states from the RIXS curves with good data statistics ($E_4 = 105.5$ eV, $E_7 = 110.4$ eV, $E_9 = 122.2$ eV, and $E_{10} = 125$ eV) are fitted by two peaks. Black circles are experimental data and red curves are the cumulative peaks' fitting results.

together could interpret the two excitation peaks in the $J = 7/2$ states. If so, the tiny gap between Γ_8' and Γ_6' might not be easily distinguished, and only one merged large peak can be detected due to the limited apparatus energy resolution (∼15 meV). Then, a detailed fitting of the upper branch excitations with two peaks is shown in Figs. 4(a)–4(c). The overall fitting quality is acceptable, despite possibly missing some spikes around the two main peaks. The extracted CEF split energy from the dual-peak fitting within $J = 7/2$ is approximately 77 meV, which is smaller than the result of 82 meV from Raman scattering. However, by analyzing the fitting details, one could find that the full width at half maximum (FWHM) value of peak 3 ($\Gamma_8' + \Gamma_6'$) is extraordinarily large, even twice its counterpart in peak 4 (Γ_7'), as shown in Fig. 4(b). Although the fourfold degeneracy of quadruplet Γ_8' naturally bears a broadened excitation peak than the doubly degenerate Γ_7', the dispute cannot be reconciled because the second-order split within Γ_8' and Γ_7' is sub-meV (∼10 K) and it would not profoundly impact the excitation width. That means peak 3 should present two well-separated excitations, and thus dual-peak fitting is problematic and misleading by assuming Γ_8' and Γ_6' are located coincidently in energy.

The discussion above proposes that the RIXS line profile of $J = 7/2$ excitations deserves a better analysis than naive dual-peak fitting, and the Γ_6' and Γ_8' states of $J = 7/2$ should be distinguishable under the fitting. Therefore, a fitting of $J = 7/2$ excitations with three peaks is also presented in Figs. 4(d)–4(f). The overall fitting quality is significantly improved and the sum of squares (SS) value has been shrunk to one order of magnitude smaller than the dual-peak fitting. More importantly, the fitting details of peaks are now much

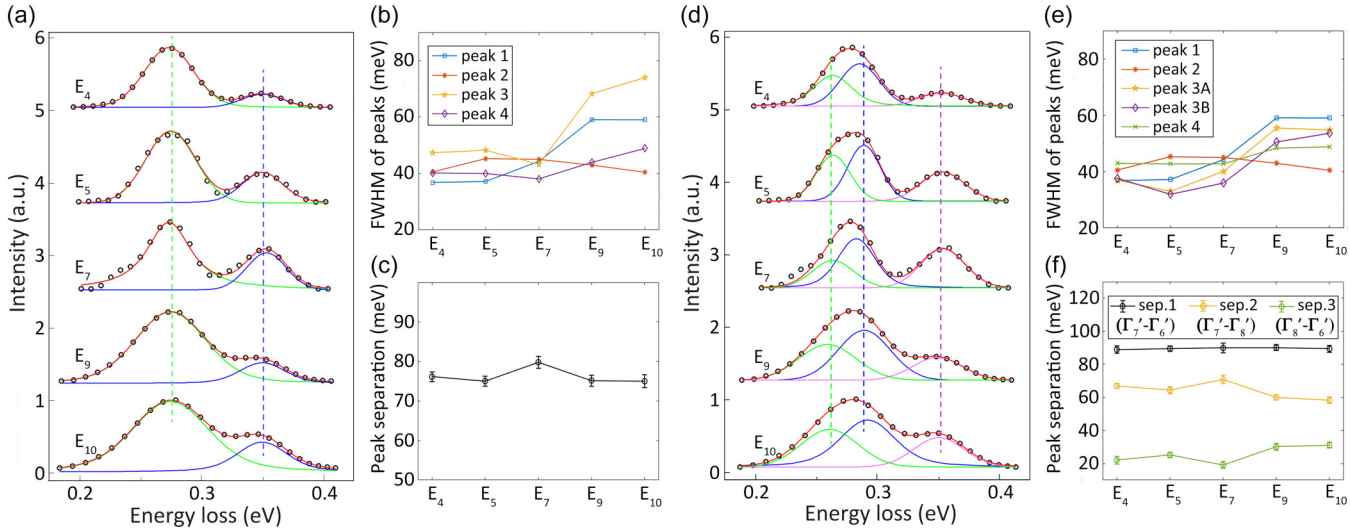

FIG. 4. (a) The inelastic emission of the $J = 7/2$ states from the RIXS curves with good data statistics ($E_4 = 105.5$ eV, $E_5 = 106.4$ eV, $E_7 = 110.4$ eV, $E_9 = 122.2$ eV, and $E_{10} = 125$ eV) is fitted by two peaks. Black circles are experimental data and red curves are the cumulative peaks' fitting results. (b) The FWHM values of the fitted peaks extracted from (a) and two fitted peaks in the $J = 5/2$ state. The four peaks represent the elastic peak (peak 1) and the excitation from the ground state to Γ_7 (peak 2), $\Gamma_6' + \Gamma_8'$ (peak 3), and Γ_7' (peak 4). (c) The total CEF split within the $J = 7/2$ state, extracted from the energy separation between peak 3 and peak 4 in (a). (d) The fitting of RIXS curves with three peaks, representing the excitation from Γ_8 to Γ_6' (peak 3A), Γ_8' (peak 3B), and Γ_7' (peak 4). (e) The FWHM values of the fitted peaks extracted from (e) and two fitted peaks in the $J = 5/2$ state. (f) The extracted total CEF split within the $J = 7/2$ state, extracted from the energy separation between peak 3A and peak 4 in (d).

more reasonable. For instance, the FWHM of every peak is now rather comparable to each other, correcting the errors in the dual-peak fitting that one peak is overwhelmingly broader than the others [Fig. 4(e)]. Still, peak 3B, which is attributed to the quadruplet Γ_8' states ($J = 7/2$), possesses more intensity than peak 3A (doublet Γ_6') and peak 4 (doublet Γ_7'). The fitting-extracted energy split between the Γ_6' and Γ_8' is about 25 meV, which is also larger than the value of 14 meV reported in Raman scattering. In addition, the CEF split between the Γ_7' and Γ_8' is about 65 meV, nearly identical to the Raman scattering result. Together, the fitting gives an overall CEF split of 89.5 meV within the $J = 7/2$ states [Fig. 4(f)]. The CEF value of 89.5 meV extracted from our RIXS data is about 10% larger than the value of 82 meV from the Raman experiment. However, it is not necessary to draw a conclusion that either value is more accurate unless the following considerations are clearly resolved.

First, the divergence could be a direct result of the difference between these two experimental techniques. It has also been reported in other research that the excitation energy probed by RIXS could be larger than the ones from Raman scattering. As an example, the first-order vibration mode in water's O-H band probed by RIXS shows an apparent blueshift when compared with the result of Raman scattering. [44–46]. Although both techniques are based on scattering, Raman scattering is related to the nonresonant process, while the RIXS relies on energy resonance.

The conflicts may also be intrinsically linked to the less metallic nature of the heavily alloyed Ce/SmB_6. Previous magnetic susceptibility measurements and our XAS measurements support the dominance of the $4f^1$ valence state in the alloyed compound, and substituting with Sm would not change the lattice configuration of B_6 cages surrounding the Ce site. However, it is noteworthy that CEF is raised from the molecular orbital model, which is highly associated with an insulating picture and would be blurred by the quasiparticle dispersions and enhanced bandwidth. Instead of the insulating SmB_6 [47,48], CeB_6 is a Kondo metal [7,49]. Heavily alloying Ce with Sm would depress the itinerancy in CeB_6, which enhances the energy scale of CEF. The cooling down of CeB_6 makes it more insulating, but with larger CEF splitting. This effect could also be realized in the temperature-dependent Raman data in Refs. [35,50].

IV. CONCLUSION

In this paper, we precisely depicted the energy scales of CEF symmetries by using high-resolution RIXS. Our result suggests a larger CEF split of 89.5 meV in the $J = 7/2$ states when comparing our findings with a recent Raman spectroscopy work. With respect to the discrepancy, it cannot be excluded as a result associated with the alloying with Sm (intrinsic) or the difference of the scattering process (extrinsic). Although further study is necessary to reconcile the dispute between our result with the previous one, our work constitutes another piece of evidence for the theoretical community and hopefully provides insights into strongly correlated systems with a Ce $4f^1$ basis. As already mentioned, the CEF split ground state symmetry and the framework of CEF energy hierarchy give the basis for comprehending the electronic correlations and the nontrivial topology in the heavy fermion material $Ce_{0.3}Sm_{0.7}B_6$. For example, the value of CEF could signal the bandwidth, itineracy, as well as hybridization between the f-orbital and other bands. Thus, an accurate CEF energy level would put an explicit constraint on the first-

principles calculation, which would generate a theoretical treatment much closer to the underlying physics.

ACKNOWLEDGMENTS

L.M. was supported by the National Natural Science Foundation of China (Grants No. U2032156 and No. 12004071), Natural Science Foundation of Jiangsu Province, China (Grant No. BK20200348), Ministry of Science and Technology of China (Grant No. 2022YFA1405700), and the program of Jiangsu specially-appointed professor. L.A.W. acknowledges the support of the National Science Foundation under Grant No. DMR-2105081. This research used resources of the Advanced Light Source, a U.S. DOE Office of Science User Facility under Contract No. DE-AC02-05CH11231.

[1] K. N. Lee and B. Bell, Phys. Rev. B **6**, 1032 (1972).
[2] K. Haule, C.-H. Yee, and K. Kim, Phys. Rev. B **81**, 195107 (2010).
[3] Q. Y. Chen, D. F. Xu, X. H. Niu, R. Peng, H. C. Xu, C. H. P. Wen, X. Liu, L. Shu, S. Y. Tan, X. C. Lai, Y. J. Zhang, H. Lee, V. N. Strocov, F. Bisti, P. Dudin, J.-X. Zhu, H. Q. Yuan, S. Kirchner, and D. L. Feng, Phys. Rev. Lett. **120**, 066403 (2018).
[4] C. K. Barman, P. Singh, D. D. Johnson, and A. Alam, Phys. Rev. Lett. **122**, 076401 (2019).
[5] Q. Yao, D. Kaczorowski, P. Swatek, D. Gnida, C. H. P. Wen, X. H. Niu, R. Peng, H. C. Xu, P. Dudin, S. Kirchner, Q. Y. Chen, D. W. Shen, and D. L. Feng, Phys. Rev. B **99**, 081107(R) (2019).
[6] D. Hafner, P. Khanenko, E.-O. Eljaouhari, R. Küchler, J. Banda, N. Bannor, T. Lühmann, J. F. Landaeta, S. Mishra, I. Sheikin, E. Hassinger, S. Khim, C. Geibel, G. Zwicknagl, and M. Brando, Phys. Rev. X **12**, 011023 (2022).
[7] T. Komatsubara, N. Sato, S. Kunii, I. Oguro, Y. Furukawa, Y. Ōnuki, and T. Kasuya, J. Magn. Magn. Mater. **31**, 368 (1983).
[8] E. Zirngiebl, B. Hillebrands, S. Blumenröder, G. Güntherodt, M. Loewenhaupt, J. M. Carpenter, K. Winzer, and Z. Fisk, Phys. Rev. B **30**, 4052 (1984).
[9] F. Steglich, J. Aarts, C. D. Bredl, W. Lieke, D. Meschede, W. Franz, and H. Schäfer, Phys. Rev. Lett. **43**, 1892 (1979).
[10] W. Assmus, M. Herrmann, U. Rauchschwalbe, S. Riegel, W. Lieke, H. Spille, S. Horn, G. Weber, F. Steglich, and G. Cordier, Phys. Rev. Lett. **52**, 469 (1984).
[11] C. Petrovic, P. Pagliuso, M. Hundley, R. Movshovich, J. Sarrao, J. Thompson, Z. Fisk, and P. Monthoux, J. Phys.: Condens. Matter **13**, L337 (2001).
[12] Y. Ōnuki, Y. Shimizu, M. Nishihara, Y. Machii, and T. Komatsubara, J. Phys. Soc. Jpn. **54**, 1964 (1985).
[13] H. Sato, I. Sakamoto, K. Yonemitsu, Y. Ōnuki, T. Komatsubara, Y. Kaburagi, and Y. Hishiyama, J. Magn. Magn. Mater. **52**, 357 (1985).
[14] A. P. Pikul, U. Stockert, A. Steppke, T. Cichorek, S. Hartmann, N. Caroca-Canales, N. Oeschler, M. Brando, C. Geibel, and F. Steglich, Phys. Rev. Lett. **108**, 066405 (2012).
[15] J. Effantin, J. Rossat-Mignod, P. Burlet, H. Bartholin, S. Kunii, and T. Kasuya, J. Magn. Magn. Mater. **47**, 145 (1985).
[16] M. Kawakami, S. Kunii, T. Komatsubara, and T. Kasuya, Solid State Commun. **36**, 435 (1980).
[17] G. Friemel, Y. Li, A. Dukhnenko, N. Y. Shitsevalova, N. Sluchanko, A. Ivanov, V. Filipov, B. Keimer, and D. Inosov, Nat. Commun. **3**, 830 (2012).
[18] M. Sera, N. Sato, and T. Kasuya, J. Magn. Magn. Mater. **63**, 64 (1987).
[19] A. S. Cameron, G. Friemel, and D. S. Inosov, Rep. Prog. Phys. **79**, 066502 (2016).
[20] W. Erkelens, L. Regnault, P. Burlet, J. Rossat-Mignod, S. Kunii, and T. Kasuya, in *Anomalous Rare Earths and Actinides* (Elsevier, Amsterdam, 1987), pp. 61–63.
[21] S. Nakamura, T. Goto, and S. Kunii, J. Phys. Soc. Jpn. **64**, 3941 (1995).
[22] S. Yeo, K. Song, N. Hur, Z. Fisk, and P. Schlottmann, Phys. Rev. B **85**, 115125 (2012).
[23] M. Ciomaga Hatnean, T. Ahmad, M. Walker, M. R. Lees, and G. Balakrishnan, Crystals **10**, 827 (2020).
[24] O. Erten, P.-Y. Chang, P. Coleman, and A. M. Tsvelik, Phys. Rev. Lett. **119**, 057603 (2017).
[25] A. Koitzsch, N. Heming, M. Knupfer, B. Büchner, P. Portnichenko, A. Dukhnenko, N. Shitsevalova, V. Filipov, L. Lev, V. Strocov *et al.*, Nat. Commun. **7**, 10876 (2016).
[26] P. Y. Portnichenko, A. Akbari, S. E. Nikitin, A. S. Cameron, A. V. Dukhnenko, V. B. Filipov, N. Y. Shitsevalova, P. Čermák, I. Radelytskyi, A. Schneidewind, J. Ollivier, A. Podlesnyak, Z. Huesges, J. Xu, A. Ivanov, Y. Sidis, S. Petit, J.-M. Mignot, P. Thalmeier, and D. S. Inosov, Phys. Rev. X **10**, 021010 (2020).
[27] L. Miao, C.-H. Min, Y. Xu, Z. Huang, E. C. Kotta, R. Basak, M. S. Song, B. Y. Kang, B. K. Cho, K. Kißner, F. Reinert, T. Yilmaz, E. Vescovo, Y.-D. Chuang, W. Wu, J. D. Denlinger, and L. A. Wray, Phys. Rev. Lett. **126**, 136401 (2021).
[28] Y. Xu, E. C. Kotta, M. S. Song, B. Y. Kang, J. W. Lee, B. K. Cho, S. Liu, T. Yilmaz, E. Vescovo, J. D. Denlinger, L. Miao, and L. A. Wray, Phys. Rev. B **104**, 115118 (2021).
[29] M. Sundermann, K. Chen, H. Yavaş, H. Lee, Z. Fisk, M. Haverkort, L. H. Tjeng, and A. Severing, Europhys. Lett. **117**, 17003 (2017).
[30] L. Hu, M. F. Reid, C.-K. Duan, S. Xia, and M. Yin, J. Phys.: Condens. Matter **23**, 045501 (2011).
[31] P. A. Tanner, C. S. Mak, N. M. Edelstein, K. M. Murdoch, G. Liu, J. Huang, L. Seijo, and Z. Barandiarán, J. Am. Chem. Soc. **125**, 13225 (2003).
[32] T. Takahashi, T. Morimoto, T. Yokoya, S. Kunii, T. Komatsubara, and O. Sakai, Phys. Rev. B **52**, 9140 (1995).
[33] S. Horn, F. Steglich, M. Loewenhaupt, H. Scheuer, W. Felsch, and K. Winzer, Z. Phys. B **42**, 125 (1981).
[34] B. Löthi, S. Blumenröder, B. Hillebrands, E. Zirngiebl, G. Güntherodt, and K. Winzer, Z. Phys. B **58**, 31 (1984).
[35] M. Ye, H.-H. Kung, P. F. S. Rosa, E. D. Bauer, Z. Fisk, and G. Blumberg, Phys. Rev. Mater. **3**, 065003 (2019).
[36] See Supplemental Material at http://link.aps.org/supplemental/10.1103/PhysRevB.107.245149 for additional information about the RIXS data of the CeB_6 sample, and the atomic multiplet simulations on Ce $4f^1$ and Sm $4f^5/4f^6$ configurations, which includes Ref. [38].

[37] L. A. Wray, J. Denlinger, S.-W. Huang, H. He, N. P. Butch, M. B. Maple, Z. Hussain, and Y.-D. Chuang, Phys. Rev. Lett. **114**, 236401 (2015).

[38] H. He, L. Miao, E. Augustin, J. Chiu, S. Wexler, S. A. Breitweiser, B. Kang, B. K. Cho, C.-H. Min, F. Reinert, Y.-D. Chuang, J. Denlinger, and L. A. Wray, Phys. Rev. B **95**, 195126 (2017).

[39] K. J. Kormondy, L. Gao, X. Li, S. Lu, A. B. Posadas, S. Shen, M. Tsoi, M. R. McCartney, D. J. Smith, J. Zhou *et al.*, Sci. Rep. **8**, 7721 (2018).

[40] P. Tieu, X. Yan, M. Xu, P. Christopher, and X. Pan, Small **17**, 2006482 (2021).

[41] M. Magnuson, S. M. Butorin, J.-H. Guo, A. Agui, J. Nordgren, H. Ogasawara, A. Kotani, T. Takahashi, and S. Kunii, Phys. Rev. B **63**, 075101 (2001).

[42] A. Kotani and S. Shin, Rev. Mod. Phys. **73**, 203 (2001).

[43] S. Souma, H. Kumigashira, T. Ito, T. Sato, T. Takahashi, and S. Kunii, J. Electron Spectrosc. Relat. Phenom. **114**, 729 (2001).

[44] D. Mariedahl, F. Perakis, A. Späh, H. Pathak, K. H. Kim, C. Benmore, A. Nilsson, and K. Amann-Winkel, Philos. Trans. R. Soc. A **377**, 20180164 (2019).

[45] E. J. Jaeschke, S. Khan, J. R. Schneider, and J. B. Hastings, *Synchrotron Light Sources and Free-Electron Lasers: Accelerator Physics, Instrumentation and Science Applications* (Springer, Berlin, 2016).

[46] V. Vaz da Cruz, F. Gel'mukhanov, S. Eckert, M. Iannuzzi, E. Ertan, A. Pietzsch, R. C. Couto, J. Niskanen, M. Fondell, M. Dantz *et al.*, Nat. Commun. **10**, 1013 (2019).

[47] T. Kasuya, Europhys. Lett. **26**, 277 (1994).

[48] J. C. Cooley, M. C. Aronson, Z. Fisk, and P. C. Canfield, Phys. Rev. Lett. **74**, 1629 (1995).

[49] M. Neupane, N. Alidoust, I. Belopolski, G. Bian, S.-Y. Xu, D.-J. Kim, P. P. Shibayev, D. S. Sanchez, H. Zheng, T.-R. Chang, H.-T. Jeng, P. S. Riseborough, H. Lin, A. Bansil, T. Durakiewicz, Z. Fisk, and M. Z. Hasan, Phys. Rev. B **92**, 104420 (2015).

[50] C. Terzioglu, D. A. Browne, R. G. Goodrich, A. Hassan, and Z. Fisk, Phys. Rev. B **63**, 235110 (2001).